

ϕ - meson Production at RHIC energies using the PHENIX Detector

Deepali Sharma (For the PHENIX Collaboration)

Department of Particle Physics, The Weizmann Institute of Science, Rehovot, 76100, Israel

E-mail: deepali.sharma@weizmann.ac.il

Abstract. Light vector mesons are among the most informative probes to understand the strongly coupled Quark Gluon Plasma created at RHIC. The suppression of light mesons at high transverse momentum, compared to expectations from scaled $p + p$ results, reflects the properties of the strongly interacting matter formed. The ϕ -meson is one of the probes whose systematic measurement in $p + p$, $d + Au$ and $Au + Au$ collisions can provide useful information about initial and final state effects on particle production. The mass, width and branching ratio of the ϕ -meson decay in the di-kaon and di-electron decay channels could be modified in $Au + Au$ collisions due to the restoration of chiral symmetry in the QGP.

The PHENIX experiment at RHIC has measured ϕ -meson production in various systems ranging from $p + p$, $d + Au$ to $Au + Au$ collisions via both its di-electron and di-kaon decay modes. A summary of PHENIX results on invariant spectra, nuclear modification factor and elliptic flow of the ϕ -meson are presented here.

1. Introduction

The ϕ - meson plays a unique role in the study of the hot and dense medium created in relativistic heavy-ion collisions. It is the lightest bound state of hidden strangeness $s\bar{s}$, has a small interaction with other non-strange hadrons and hence carries information from the early partonic stages of the system evolution. Comparing the elliptic flow (v_2) of ϕ to the v_2 of other multistrange hadrons (Ω and Ξ) or particles composed of lighter quarks (u and d) or heavier charm quark, provides information about the partonic collectivity of the medium.

Furthermore the ϕ can provide important information on particle production mechanisms, since it is a meson but has a mass similar to p and Λ baryons. The measurement of its nuclear modification factor, R_{AA} adds to the picture of particle suppression and its dependence on particle mass and composition supporting hydrodynamics and recombination models.

The ϕ can also be sensitive to the restoration of chiral symmetry. A certain fraction of the ϕ can decay inside the hot and dense media leading to a change in its spectral function[1, 2]. This modification can be seen by studying the low-momentum ϕ decaying inside the media and reconstructed via the di-electron decay channel. Since leptons are not subject to the strong interaction, they preserve their production information. A change in mass or width (Γ) of ϕ inside the medium can lead to a change in the relative branching ratios of the $\phi \rightarrow K^+K^-$ and $\phi \rightarrow e^+e^-$ decay modes. Since $m_\phi \approx 2 \times m_K$, small changes in ϕ or K can induce significant changes in the branching ratio.

2. The PHENIX Detector

The PHENIX detector[3] at RHIC (Relativistic Heavy Ion Collider) has been designed to measure both leptons and hadrons. A schematic view of the PHENIX detector is shown in Fig. 1. Each of the two central arm spectrometers covers 90° in azimuth and ± 0.35 in pseudorapidity and has the capability to measure neutral and charged particles. The high-resolution multi-wire proportional Drift Chambers (DC) together with the first layer of Pad Chambers (PC1) provide the charged particle tracking and momentum measurement. The typical momentum resolution is $\sigma(p_T)/p_T \approx 1.0\%p_T \oplus 1.1\%$.

The Kaons are identified by using the timing information from a high resolution Time of Flight (TOF) detector and the Lead Scintillator (PbSc) part of the Electromagnetic Calorimeter (EMCal), with good π/K separation over the momentum range 0.3 - 2.5

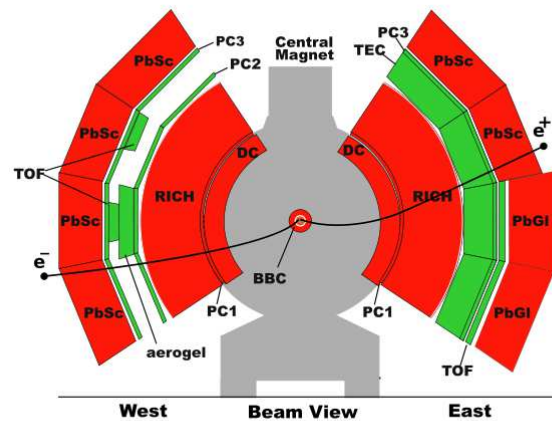


Figure 1. Schematic view of the PHENIX experiment, highlighting the subsystems used in di-electron analysis.

GeV/ c and 0.3 - 1 GeV/ c , respectively. The electrons are identified using a Ring Imaging Čerenkov Detector (RICH) and by requiring the energy measured in the EMCal to match the measured momentum of the charged tracks in the DC. The Zero Degree Claorimeters (ZDC's) and Beam Beam Counters (BBC's) are dedicated subsystems that measure global quantities such as luminosity, collision vertex and event centrality. The minimum bias trigger is derived by a coincidence between the two BBCs; in $p + p$ and $d + Au$ the trigger requires at least one hit in each BBC arm whereas for $Au + Au$ at least two hits in each BBC arm and one detected neutron in ZDC is needed. In order to benefit from the high luminosity in $p + p$ and $d + Au$ collisions and to efficiently detect electrons, a special online EMCal RICH trigger (ERT) is used. It requires an event to have at least one track with an energy above a certain threshold in the EMCal and a geometrically correlated hit in the RICH. The results presented here correspond to the data for $p + p$ (2005), $d + Au$ (2003) and $Au + Au$ (2004) taken at $\sqrt{s_{NN}} = 200$ GeV $\sqrt{s_{NN}} = 62.4$ GeV.

3. Analysis Details

For the $\phi \rightarrow K^+K^-$ mass reconstruction, the charged tracks are combined to form pairs using three different techniques. The first one does not require any Kaon identification and assigns the kaon mass to all tracks (“No Kaon PID”). The second method requires one track to be identified as Kaon in the TOF subsystem (One Kaon “PID”), whereas the third method requires both the tracks to be identified as Kaons either in TOF or EMCal subsystems (“Two Kaon PID”). The “No Kaon PID” method allows us to go to high p_T as compared to the other two, is a relatively simpler analysis, but with comparatively large B/S ratio. The “Two Kaons PID” method allows us to go lower in p_T and has small B/S ratio. The “One Kaon PID” method has the advantage of less background and so works with better accuracy for the low p_T (< 2 GeV/ c) region where “No Kaon PID” method has a large background. The $p + p$ data was analyzed using “No Kaon PID”, and “One Kaon PID”, $d + Au$ using “No Kaon PID” and “Two Kaons PID” and $Au + Au$ using “One Kaon PID” and “Two Kaons PID”. The 62.4 GeV $Au + Au$ data was analyzed using “Two Kaons PID” method only. The different analysis methods have very different sources of systematic uncertainties and provide a valuable consistency check. In Fig. 2(a), good agreement between the various methods can be seen. The combined $p + p$ result using “One Kaon PID” and “No Kaon PID” analyses constitutes a new $p + p$ reference for ϕ -meson, surpassing the previous one[6], in p_T and with smaller errors.

For $\phi \rightarrow e^+e^-$, electrons identified using RICH and EMCal are combined in pairs to generate like- and unlike-sign mass spectra. However, due to the limited azimuthal angular acceptance and the strong magnetic field beginning at R=0, the identification and rejection of e^+e^- pairs from Dalitz decays and photon conversions is very difficult[7]. This results in a huge combinatorial background in $Au + Au$, making this measurement difficult.

Raw yields, for both K^+K^- and e^+e^- are then extracted either by simultaneously fitting the signal and background, or by integrating the spectra in the vicinity of the peak after subtraction of the combinatorial background, estimated using an event-mixing technique[4, 5]. The correction function takes into account the limited detector acceptance and resolution and reconstruction efficiency and was derived by a full single-particle Monte Carlo simulation, propagated through an emulator of the PHENIX detector and the full analysis chain. Corrections to incorporate the trigger efficiency and multiplicity effects are applied too. Fig. 2 summarizes the ϕ measurements in $p+p$, and di-electron decay modes.

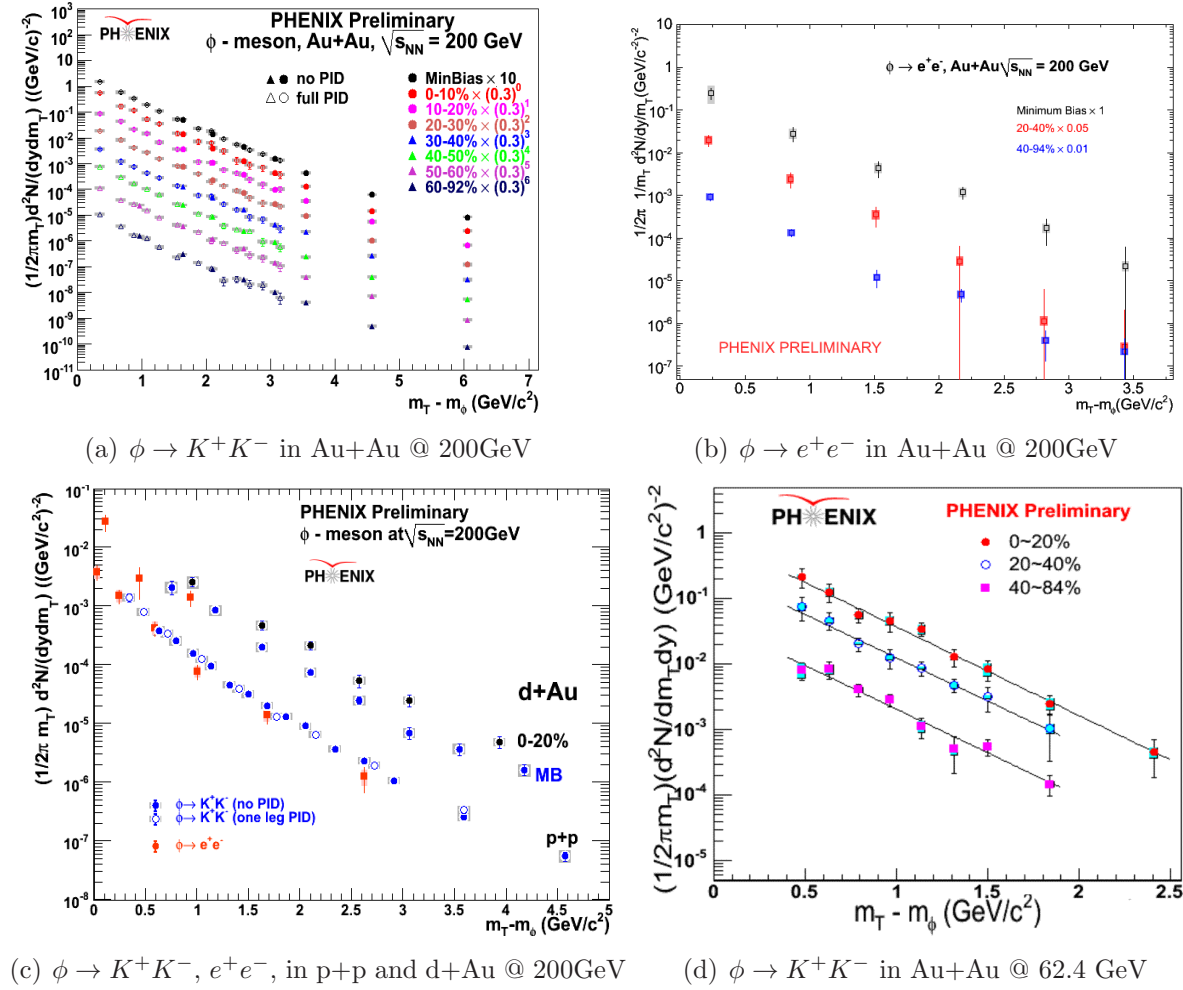


Figure 2. Invariant spectra of ϕ -meson measured in different colliding systems.

4. Results

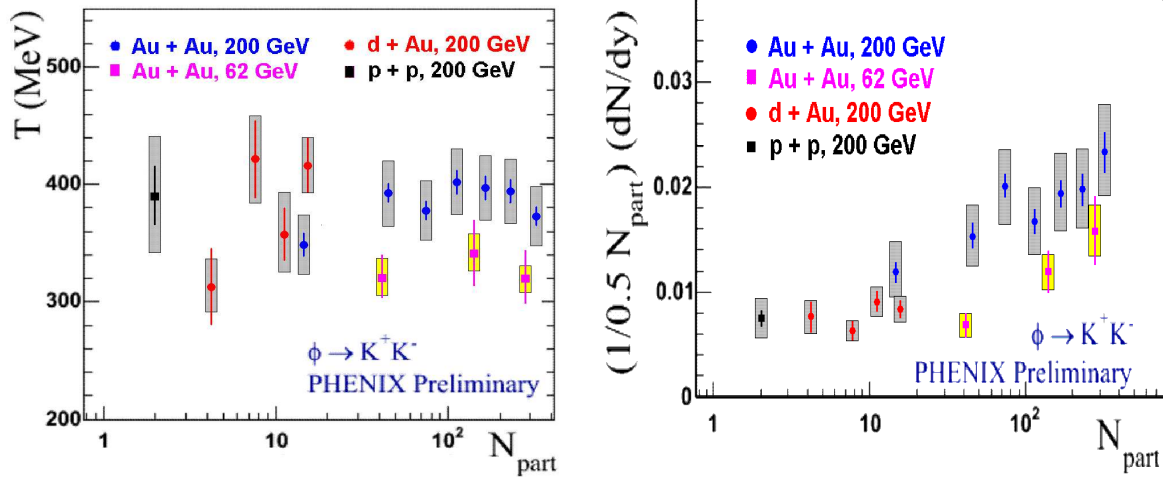
4.1. dN/dy and T

The integrated yields and temperature presented in Fig. 3 were extracted assuming m_T dependent yields to be exponential and so fitting the m_T spectra to the following

exponential function with dN/dy and T as the parameters.

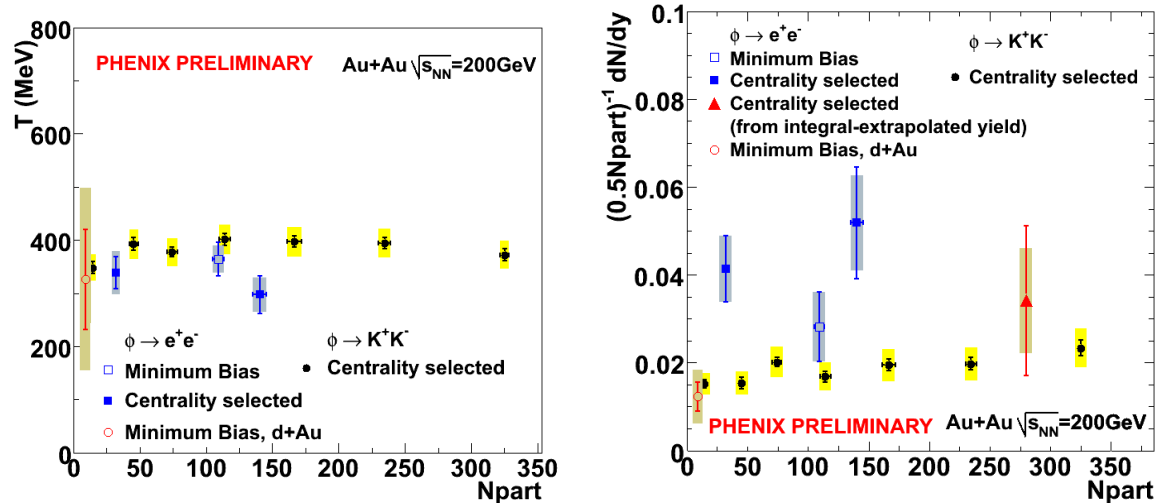
$$\frac{1}{2\pi m_T} \cdot \frac{d^2N}{dm_T dy} = \frac{dN/dy}{2\pi T(T + M_\phi)} \cdot \exp(-(m_T - M_\phi)/T) \quad (1)$$

The temperatures extracted in the two decay channels are in good agreement with each other, do not change between different collision systems but grow only slightly from 62.4 GeV to 200 GeV as can be seen in Figs. 3(a) & 3(c). The integrated yields normalized to the number of participants increase by almost a factor of two from peripheral to central $Au + Au$ collisions. Particle yields in the e^+e^- channel seem to be higher than the corresponding K^+K^- decay channel, but the large systematic and statistical uncertainties in di-electron measurement prevent us from making any conclusive statement.



(a) “T” as a function of system size and energy

(b) Normalized yields as a fn. of N_{part}



(c) “T” comparison between e^+e^- and K^+K^-

(d) dN/dy comparison between e^+e^- and K^+K^-

Figure 3. Integrated yields and Temperature

4.2. v_2 of ϕ

The v_2 of ϕ was extracted following the m_{inv} method[8], using the $K+K^-$ decay mode. A detailed description of the analysis procedure can be found in [9]. Results for v_2 as a function of KE_T for the ϕ -meson together with π^\pm , K^\pm & $(\bar{p})p$ are shown in the left (right) panel of Fig. 4 without (with) scaling with the number of valence quarks. It is clear from the left panel that despite its similar mass to the proton, $v_2(KE_T)$ for the ϕ -meson follows the flow pattern of the other lighter mesons(π and K). The right panel of the Fig. 4 shows universal scaling behavior of the elliptic flow of baryons and mesons when both v_2 and KE_T are scaled with the number of valence quarks. This indicates that the elliptic flow develops during the early stage when the constituents of the flowing medium are partons and not ordinary hadrons interacting with their standard hadronic cross-sections.

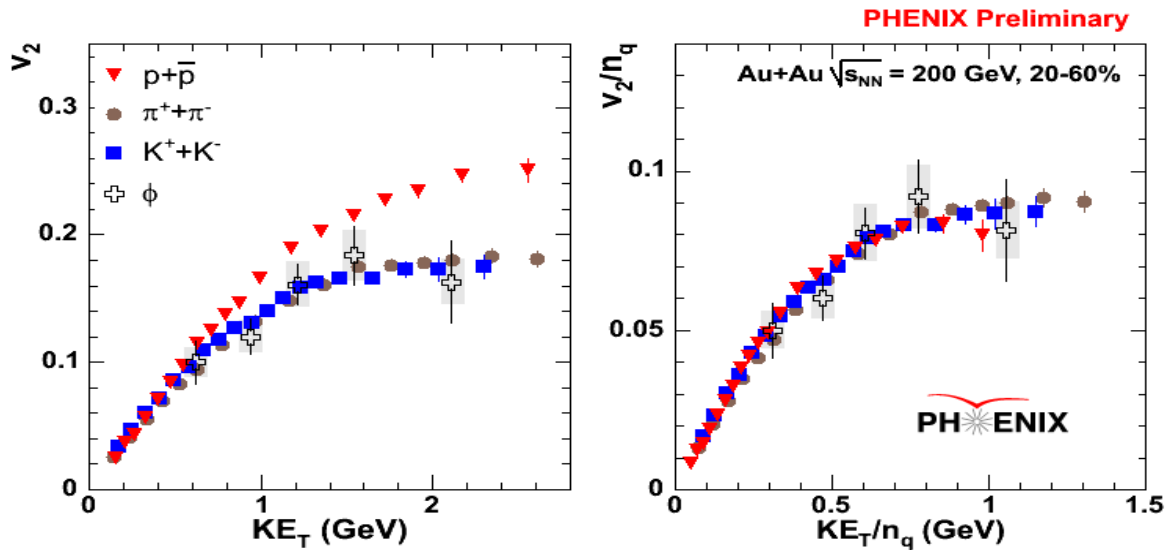


Figure 4. (a) v_2 vs KE_T for identified particles[10] in mid-central (20-60%) $Au + Au$ collisions. (b) v_2/n_q vs KE_T/n_q for the same set of particles

4.3. Nuclear Modification Factor

The nucleus-nucleus collisions at RHIC have revealed a decrease in hadron production at high p_T relative to scaled $p + p$ collisions. The nuclear medium effects on hadron production are quantified by the nuclear modification factor R_{AA} , defined as the ratio of the yield obtained from nucleus-nucleus collisions scaled down with the number of binary collisions, to the yield from elementary nucleon-nucleon collisions.

$$R_{AA}(p_T) = \frac{d^2 N^{AA}/dp_T dy}{\langle n_{coll} \rangle \cdot d^2 N^{pp}/dp_T dy} \quad (2)$$

In the absence of any nuclear effects, the ratio should saturate at unity for high p_T , where the production is dominated by hard scattering and is proportional to the number of binary collisions (N_{coll}), in contrast to low p_T region where soft processes dominate. R_{dAu} , which is the nuclear modification factor for $d + Au$ collisions helps to differentiate initial state effects from final state effects and also to study other cold nuclear matter effects. Fig.5 shows R_{dAu} measurement of the ϕ for 0-20% and minimum bias collisions plotted together with $\eta \rightarrow \gamma\gamma$ and $\pi^0 \rightarrow \gamma\gamma$ mesons for comparison. Whereas the R_{dAu} of π and η are consistent with unity, the R_{dAu} of ϕ for 0-20% shows some enhancement, but with very large error bars.

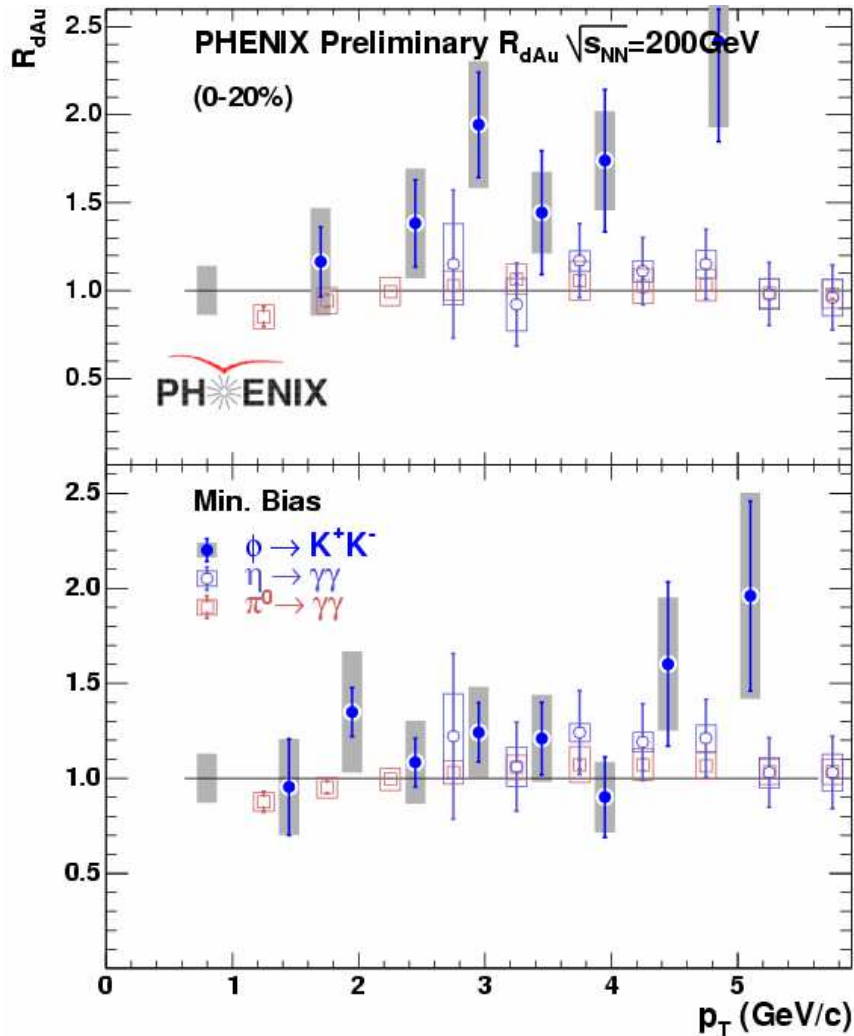


Figure 5. R_{dAu} of ϕ, η & π^0 mesons[11].

Fig.6[12] shows the nuclear modification factor for the ϕ -meson in central $Au + Au$ collisions using the new $p + p$ reference from 2005 run results, over a p_T range of 2.45 - 7 GeV/c. For comparison, the R_{AA} of direct $\gamma, \pi^0, \eta, \omega, (K^+ + K^-)/2$ & $(p + \bar{p})/2$ are also plotted. π^0 and η follow the same suppression pattern over the entire p_T range.

The ϕ -meson at intermediate p_T ($2.45 < p_T < 4.5$ GeV/ c) exhibits more suppression than the protons but less suppression than η and π^0 mesons, whereas at higher p_T (> 5 GeV/ c) the amount of suppression of ϕ and ω could be similar to that of π^0 and η . The similar suppression patterns of various mesons at high p_T support the concept of meson production via jet-fragmentation at high p_T outside the hot and dense medium created in the collisions. In the future, the comparison of extended measurements of charged Kaons with that of ϕ will give an insight into, whether or not quark flavor composition plays a role on the suppression pattern.

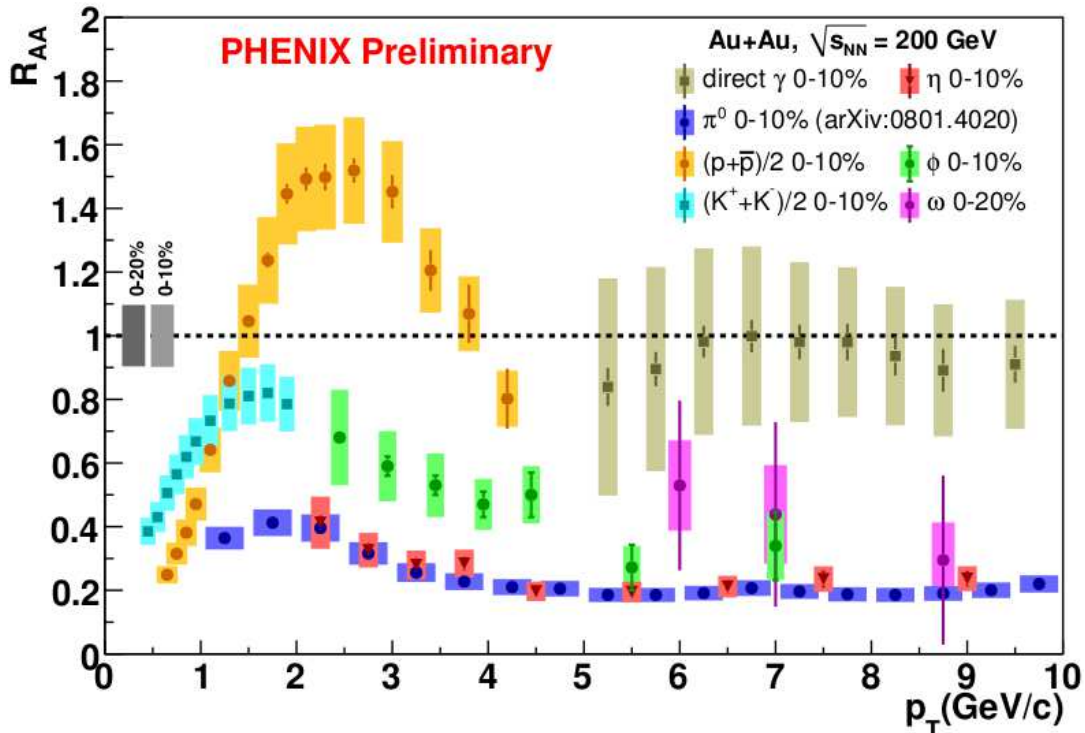


Figure 6. Nuclear modification factor R_{AA} in central Au+Au collisions as a function of p_T for π^0 , $(K^+ + K^-)/2$, η , ω , $(p + \bar{p})/2$, ϕ and direct γ .

5. Summary

The PHENIX experiment at RHIC has measured ϕ -meson production using both e^+e^- and K^+K^- in $p+p$, $d+Au$ and $Au+Au$ collisions at $\sqrt{s_{NN}} = 200$ GeV. The preliminary results in $p+p$ via both channels agree to each other. The measurements in $d+Au$ suffer from low statistics in both the channels. With the high statistics $d+Au$ data collected in year 2008, results with better precision and wide p_T coverage are expected. In $Au+Au$, the ϕ -meson has been measured via K^+K^- with good accuracy while e^+e^- measurements are expected to improve considerably with the newly installed Hadron Blind Detector[13, 14, 15] in PHENIX. The v_2 of ϕ follows the flow pattern of other

mesons as well as scales with $n_q = 2$, indicating partonic collectivity. R_{dAu} of ϕ does not show any suppression, but large error bars leave room for Cronin enhancement. The R_{AA} of ϕ shows a similar suppression pattern to that of π^0 and η at high p_T , but at intermediate p_T , the suppression level is different.

6. Acknowledgements

The author acknowledges support by the Israel Science Foundation, the MINERVA Foundation and the Nella and Leon Benozziyo Center of High Energy Physics Research.

References

- [1] S. Pal, C.M. Ko and Z. Lin, Nucl. Phys. A707, (2002) 525.
- [2] D Lissauer et al, 1991 Phys. Rev. Lett. B253 15-18.
- [3] K. Adcox et al., Nucl. Instrum. Meth. A 499 (2003) 469.
- [4] V. Ryabov, 2006 Nucl. Phys. A774 735-738.
- [5] A. Kozlov, Nucl.Phys. A774 (2006) 739-742
- [6] D.Pal et al., Nucl. Phys. A 774, 489 (2006).
- [7] A. Kozlov, Eur. Phys. J. A 31, 836-841(2007)
- [8] N. Borghini and J. Y. Ollitrault, PRC C70, 064905(2004)
- [9] PRL 99, 052301 (2007)
- [10] PRL 98, 162301 (2007).
- [11] V. Ryabov, J.Phys.G35:044030,2008.
- [12] M. Naglis, arXiv:0809.3557(nucl-ex)
- [13] I. Rainovich, Nucl.Phys.A774:903-906,2006
- [14] A. Kozlov, I. Ravinovich, L. I. Shekhtman, Z. Fraenkal, M. Inzuka and I. Tserruya, NIM A523, 345(2004)[arXiv: physics/0309013].
- [15] Z. Fraenkel et al., NIM. A546, 466(2005) [arXiv: physics/0502008].

This figure "Inv_spec_phi_pp_d_au_v5.png" is available in "png" format from:

<http://arxiv.org/ps/0901.3362v1>

This figure "Phi_ee_auai_deeps.png" is available in "png" format from:

<http://arxiv.org/ps/0901.3362v1>

This figure "dn_dy_ee_kk_auau.png" is available in "png" format from:

<http://arxiv.org/ps/0901.3362v1>

This figure "dn_dy_per_npart.png" is available in "png" format from:

<http://arxiv.org/ps/0901.3362v1>

This figure "phi_ee_au_au_62_4Gev.png" is available in "png" format from:

<http://arxiv.org/ps/0901.3362v1>

This figure "phi_au_au_200Gev.gif" is available in "gif" format from:

<http://arxiv.org/ps/0901.3362v1>

This figure "phi_au_au_200Gev.png" is available in "png" format from:

<http://arxiv.org/ps/0901.3362v1>

This figure "phi_rda.gif" is available in "gif" format from:

<http://arxiv.org/ps/0901.3362v1>

This figure "phi_rda.png" is available in "png" format from:

<http://arxiv.org/ps/0901.3362v1>

This figure "temp_ee_kk_auai.png" is available in "png" format from:

<http://arxiv.org/ps/0901.3362v1>

This figure "temp_phi_systems.png" is available in "png" format from:

<http://arxiv.org/ps/0901.3362v1>

This figure "v2phiScaleQM.gif" is available in "gif" format from:

<http://arxiv.org/ps/0901.3362v1>

This figure "v2phiScaleQM.png" is available in "png" format from:

<http://arxiv.org/ps/0901.3362v1>